

Received April 14, 2022, accepted May 5, 2022, date of publication May 10, 2022, date of current version May 18, 2022.

Digital Object Identifier 10.1109/ACCESS.2022.3174107

System Identification Based ARV-MPPT Technique for PV Systems Under Variable Atmospheric Conditions

AHMET GÜNDOĞDU 

Department of Electrical and Electronic Engineering, Batman University, 72070 Batman, Turkey


e-mail: agundogdu23@gmail.com

ABSTRACT Different tracking algorithms have been developed to obtain maximum efficiency from the PV power systems under changing atmospheric conditions. Some of these algorithms are effective under uniform irradiance, while the others are effective under partial shading conditions. In this study, a new MPPT method designed with System Identification-SI and named SI-based polynomial ARV is proposed for a PV system under uniform irradiance. The recommended method is also an adaptive reference voltage-ARV-based method. In this method, the model in which the reference voltage is obtained has a simple polynomial structure. This polynomial model has been obtained by assuming that the PV system is a nonlinear black-box type system. The input-output data, which are required for modeling, were created in MATLAB/Simulink environment. Then, by using these data with SI-Toolbox, the mathematical model of the PV system in polynomial structure giving the input-output relationship was obtained. Temperature information was used as model input, which was the generated reference voltage. Simulation studies were carried out under two different changing atmospheric scenarios; and the performance of the proposed method was analyzed. The obtained results were compared with perturb & observe-PO, incremental conductance-IC, constant voltage reference-CVR, artificial neural network-ANN-based ARV, and SI-based nonlinear ARV methods. All simulation results showed that the recommended method is simple structured, applicable, and has high performance.

INDEX TERMS Energy conversion, energy management, MPPT algorithms, photovoltaic energy, renewable energy, system identification.

NOMENCLATURE

PO	Perturbe & Observe	IPSO	Improved Particle Swarm Optimization
IC	Incremental Inductance	GA	Genetic Algorithm
CVR	Constant Voltage Reference	GWO	Gray Wolf Optimization
ARV	Adaptive Reference Voltage	ABC	Artificial Bee Colony
CC	Constant Current	ACO	Ant Colony Optimization
HC	Hill Climbing	FFA	Firefly Algorithm
PC	Parasitic Capacitance	DE	Differential Evolution
FOCV	Fractional Open Circuit Voltage	BSA	Bat Search Algorithm
FSCC	Fractional Short Circuit Current	CA	Cat Algorithm
RCC	Ripple Correlation Control	JA	Jaya Algorithm
ANN	Artificial Neural Network	GSA	Gravitational Search Algorithm
FLC	Fuzzy Logic Control	MKE	Monkey King Evolution
PSO	Particle Swarm Optimization	CS	Cuckoo Search
		BOA	Butterfly Optimization Algorithm
		MFO	Moth-Flame Optimization
		SSA	Salp Swarm Algorithm
		SFLA	Shuffled Frog Leap Algorithm

The associate editor coordinating the review of this manuscript and approving it for publication was Reinaldo Tonkoski .

FSA	Fish Swarm Algorithm	ACO-PO	Ant Colony Optimization With Perturb & Observe
CSO	Chicken Swarm Optimization	ANN-SMC	Artificial Neural Network With Sequential Monte Carlo
WDO	Wind-Driven Optimization	MGA-FFA	Modified Genetic Algorithm And Firefly Algorithm
BA	Beta Algorithm	T-GA	Taguchi Method And Genetic Algorithm
CSA	Chaotic Search Algorithm	ABC-PO	Artificial Bee Colony And Perturb & Observe Algorithm
SSM	Segmentation Search Method	ANN-PSO	Artificial Neural Network With Particle Swarm Optim.
RSM	Random Search Method	AFL-ANN	Augmented State Feedback Precise Linearization & Artificial Neural Network
PS	Pattern Search		
GSS	Gold Section Search		
FSA	Fibonacci Search Algorithm		
ESC	Extreme Seeking Control		
BN	Bayesian Network		
MRL	Memetic Reinforcement Learning		
TRL	Transfer Reinforcement Learning		
MPTA	Maximum Power Trapezium Algorithm		
ESA	Enhanced Scanning Algorithm		
CSR	Current Source Region Detection Algorithm		
TS	Tabu Search		
AV	Artificial Vision		
OCC	Optimal Current Control		
SCS	Stepped Comparison Search		
SA	Simulated Annealing		
FWA	Fireworks Algorithm		
GSO	Glowworm Swarm Optimization		
FPA	Flower Pollination Algorithm		
TLBO	Teaching Learning-Based Optimization		
MBA	Mine Blast Optimization		
WO	Whale Optimization Algorithm		
HPO	Human Psychology Optimization		
SI-ARV	System Identification-Adaptive Reference Voltage		
IC-FFA	Firefly algorithm with incremental conductance		
PO-ANN	Perturb & Observe With Adaptive Neural Network		
FWA-PO	Fireworks Algorithm With Perturb & Observe		
GWO-PO	Gray Wolf With Perturb & Observe		
BSA-PO	Bat Search Algorithm With Perturb & Observe		
PSO-PO	Particle Swarm Optimization With Perturb & Observe		
SA-PSO	Simulated Annealing With Particle Swarm Optimization		
FSA-PSO	Fish Swarm Algorithm With Particle Swarm Optimization		
JA-DE	Jaya Algorithm With Differential Evolution		
WO-DE	Whale Optimization With Differential Evolution		
PSO-SFLA	Particle Swarm Optimization With Shuffled Frog Leaping		
SA-PO	Simulated Annealing And Perturb & Observe		
DE-PSO	Differential Evolution With Particle Swarm Optimization		

I. INTRODUCTION

Due to the usage of fossil fuels and the greenhouse effect occurring in the atmosphere, global warming is increasing rapidly, glaciers are melting, the ozone layer is pierced, natural disasters occur frequently, and people lose their lives due to diseases caused by air pollution. According to the 2019 report of the International Energy Agency (IEA), global energy-related CO₂ emissions increased by 1.7% in 2018 due to increased fossil fuel consumption [1]. Because of these disadvantages, fossil fuels are accepted not to be clean and sustainable. Due to the global environment problems caused by fossil fuels in energy production and the high costs of measures taken to solve these problems, the interest and tendency to renewable energy sources have increased in recent years.

Between 2009-2019, the share of renewable energy sources used in electrical energy production increased and reached 75% [2]. As of the end of 2019, the global scale utilization capacities of these resources are as follows: Hydropower 1150 GW, wind-power 651 GW, solar-power PV 627 GW, bio-energy 139 GW, geothermal-energy 13.9 GW, concentrating solar thermal power (CSP) 6.2 GW, ocean-power 0.5 GW.

PV power systems have advantages; for example, they are clean energy sources and environmentally friendly [3], lack of moving parts, cause no noise pollution, do not need long periodic maintenance periods, and have a life span of more than 20 years [4]. Contrary to these advantages, the efficiency of PV panels is low. To get a better result about this low efficiency, numerous studies have been carried out in the field of materials. The efficiency of silicon-based and monocrystalline standard PV panels produced with current material technology is approximately 14-17.5% under standard test conditions (Standard Test Conditions-STC-1000 W/m², 25 °C). Using the mineral called perovskite with crystal structure of ABX₃, which is in the sub-class of oxide minerals, 31% efficiency was obtained [5]. By using gallium arsenide instead, the yield could be increased up to 40%. However, this is a very costly method. The optimum operating point is called as Maximum Power Point-MPP. Different Maximum Power Point Tracking-MPPT algorithms have been

developed for the PV power system, which has low efficiency under changing conditions to operate with both high performance and maximum efficiency at the highest power-point [4]. Advances in power electronics and microprocessors have made it possible to apply many different MPPT techniques.

In this study, a new MPPT method designed with System Identification-SI is proposed. The proposed method is also an Adaptive Reference Voltage-ARV-based method, and the model, in which the reference voltage is obtained, has a simple polynomial structure. Therefore, it is named SI-based polynomial ARV. The proposed method was compared with Perturb & Observe-PO, Incremental Conductance-IC, Constant Voltage Reference-CVR, Artificial Neural Network-ANN based ARV, and SI-based nonlinear ARV methods. Simulation studies in MATLAB/Simulink environment were performed under two different changing atmospheric scenarios. After that, performance analysis of the proposed method was made. All simulation results obtained are presented in graphs comparatively.

II. CLASSIFICATION OF MPPT METHODS AND LITERATURE REVIEW

MPPT controllers play a vital role in monitoring the maximum power-point to increase the efficiency of PV systems [6]. The first PV system with MPPT was designed in 1968 for a space system [7], [8]. Numerous MPPT algorithms have been proposed and used in PV systems until today [9]. However, the performance of these different techniques to carry out comprehensive comparison by various evaluation criteria such as efficiency [10], monitoring speed [11], accuracy [6], and implementation complexity [12] is difficult. The behavior of the PV system entirely depends on the operating conditions. Therefore, analyzes, comparisons, and classifications on MPPT techniques are insufficient without considering different operating conditions [13]. Examples include the lack of methods that can be adapted to all working conditions [14], inadequate analysis of various methods [15], and uncertain classification [16].

MPPT methods are classified in different ways in the literature. A total of 62 MPPT methods developed with their modifications in [13] are categorized into seven separate groups. These are conventional algorithms, meta-heuristic algorithms, hybrid algorithms, mathematics-based algorithms, artificial intelligence-AI algorithms, algorithms based on the estimation of characteristics curves, and other algorithms. However, in reference [17], it is classified in 3 separate groups as conventional, intelligent and optimization.

Conventional MPPT methods are basically structured also easily applicable methods. These methods only follow the MP point of PV systems under uniform insolation. Therefore, under rapidly changing atmospheric conditions and partial shading conditions (PSC), they cannot observe the global maximum power point (GMPP). They fall short. Even if they catch the GMP point, they cause large oscillations that can lead to power losses with low tracking

accuracy over a long period. To overcome this disadvantage, more advanced and durable techniques have been developed. Perturb & Observe-PO [18], [19], Incremental Conductance-IC [20], [21], Constant Voltage-CV [22], [23], Adaptive Reference Voltage-ARV [24], Constant Current-CC [25], [26], Hill Climbing-HC [27], [28], Parasitic Capacitance-PC [7.29], Fractional Open Circuit Voltage-FOCV [30], Fractional Short Circuit Current-FSCC [31], Ripple Correlation Control-RCC [32], DC-Link Capacitor Drop [33], [34], On-Line MPP [35], Lookup Table [36], Linearization-based MPPT [37], [38] are the conventional MPPT methods [39], [17]. Among them, PO, IC, CV, and ARV methods are widely used.

The PO method has always been the focus of attention for researchers with its simplicity and easy applicability. Power fluctuations made by PO and similar methods at MP points are inevitable [40], [41]. In the source [42], [43], the oscillations at the MP point were reduced with a developed lock-on mechanism. The developed method was experimentally carried out under different irradiance values. A new method has been proposed by Abdel-Salam *et al.* In reference [18], it has been used for cases where PO method fails. The success of the technique under different atmospheric conditions has been demonstrated. With an extended adaptive PO algorithm proposed in [19], both steady-state power fluctuations were reduced, and also the maximum power point could be followed under partial shading conditions. In [44], a new PO method including current changes in the traditional PO method was proposed. The superiority of the proposed method was emphasized with the simulation studies. In [45], PO and IC methods were tested under dynamic environmental conditions. As a result of the tests carried out in EN 50530 standards, it was emphasized that IC method is slightly more efficient than PO method.

Regarding IC method, in [46], a modified IC method whose step changes are estimated by Fuzzy Logic was compared in detail with the traditional IC method. The superiority of the proposed method was proven by experimental studies. In [47], the success of a variable step IC method was demonstrated by simulation and experimental studies. In [48], an alternative to the variable step IC method was presented with a new technique consisting of tables. The success of the method was supported by experimental studies. In [49], a variable step IC algorithm that automatically adjusts the step size was proposed. This method, which is simple in structure and can be easily performed in digital signal processors, was confirmed by experimental studies and theoretical analysis. It has been observed that the proposed method increases MPPT speed and accuracy effectively. In [50], [51], a new IC method was proposed. It increased the monitoring speed by adjusting the duty period of DC-DC converter. For testing the effectiveness of the method, various simulation studies and experimental applications were carried out under partial shadowing and load change. The results showed that the proposed algorithm can accurately track GMP point under partial shading conditions and respond faster to changes in load and

irradiance. In [52], the efficiency of the system was increased by reducing the fluctuations around the working point with an advanced IC algorithm based on the mathematical residue theorem. The method is independent of the system parameters. In [88], a modified incremental conductance algorithm, which could respond more accurately when the irradiance level increased, was proposed and experimentally verified. Thanks to the proposed algorithm, a smoother power was achieved and lower-amplitude oscillations occurred around the maximum power point. In [89], to allow PV system to respond quickly depending on solar irradiance and load resistance that show rapid change, a high-efficiency fast-converging MPPT method was proposed. In the proposed method, to achieve rapid response, the relationship between the load line and I–V curve was determined by the trigonometry rule. Extra control loop and intermittent disconnection were eliminated.

Regarding CV method, in the reference [22], the continuous and transient state behaviors of the method were analyzed; and the efficiency of the method was investigated in depth with simulations and experimental studies. Also, a new two-mode MPPT algorithm was obtained by combining it with IC method. In [23], a new method with high performance, whose PI controller coefficients are determined by a genetic algorithm, was proposed. The efficiency and time response of the method were examined. In [53], a compensation method was presented to improve the performance of CV method. With this method, a great improvement was achieved in the controller performance. In [54], a new MPPT method obtained by combining CV and IC methods was developed to eliminate the disadvantage of CV method. The superiority of the new method used was demonstrated by the simulation study. In [55], the performance of an induction motor fed by PV system was compared using CV and other methods. In [56], the effects of CV method on PV irrigation system performed experimentally with dSpace-DS1104 controller card were examined in detail. MP point was successfully followed without oscillation in the continuous regime.

Regarding ARV method, a reference voltage table was created for ARV according to temperature and irradiance values in reference [24]. The difference between the measured voltage and the reference voltage was processed by PI controller. As a result, the duty period of the switching element was obtained. In [57], a new SI-based ARV method with a nonlinear structure that works with high performance under changing atmospheric conditions was developed by Celikel and Gundogdu.

A new CC method was proposed in [25] where short circuit current was applied at short intervals to capture GMP point under partial shading. For validating the method, a state-space-based PV system model was created, and simulation results were presented. In [27], a method that determines the update frequency of HC algorithm was presented to monitor the continuously changing MP point depending on the changing atmospheric conditions. The proposed method also revealed the relationship between perturbation step size and

energy loss. In [29], a new technique was proposed to find MP point and eliminate the parasitic capacitance effect by using the voltage fluctuations created by DC-DC converter.

Advanced MPPT methods have superior tracking performance, although they are more complex. They are preferred because they are robust, flexible, and reliable. They have been developed to overcome the disadvantages of conventional methods. Advanced methods generally include Soft Computing-SC, Evolutionary Algorithms-EA, and Artificial Intelligence-AI-based algorithms. Among these, the techniques that are widely used are as follows: Artificial neural network-ANN, fuzzy logic control-FLC, particle swarm optimization-PSO, improved particle swarm optimization-IPSO, genetic algorithm-GA, gray wolf optimization-GWO, artificial bee colony-ABC, ant colony optimization-ACO, firefly algorithm-FFA, differential evolution-DE, bat search algorithm-BSA, cat algorithm-CA, Jaya algorithm-JA, gravitational search algorithm-GSA, monkey king evolution-MKE, cuckoo search-CS, butterfly optimization algorithm-BOA, moth-flame optimization-MFO, salp swarm algorithm-SSA, shuffled frog leap algorithm-SFLA, fish swarm algorithm-FSA, chicken swarm optimization-CSO, wind-driven optimization-WDO, beta algorithm-BA, chaotic search algorithm-CSA, fibonacci search algorithm-FSA, segmentation search method-SSM, random search method-RSM, pattern search-PS, gold section search-GSS, extreme seeking control-ESC, bayesian network-BN, memetic reinforcement learning-MRL, transfer reinforcement learning-TRL, maximum power trapezium algorithm-MPTA, enhanced scanning algorithm-ESA, current source region detection algorithm-CSR, tabu search-TS, artificial vision-AV, optimal current control-OCC, stepped comparison search-SCS, simulated annealing-SA, fireworks algorithm-FWA, glowworm swarm optimization-GSO, flower pollination algorithm-FPA, teaching learning-based optimization-TLBO, mine blast optimization-MBA, whale optimization algorithm-WO, human psychology optimization-HPO [6], [13], [39]. In [58], the superiority of the FLC-based method over traditional methods is shown in comparison with the simulations made in PSIM and MATLAB/Simulink. ANN theory has increased its relevance with studies conducted in industry, PV systems, electric machines, and robotic systems [59], [60], [61]. An ANN-based MPPT algorithm has been developed for PV irrigation system with a PMSM motor in [62]. An MPPT method has been developed using Radial Basis Function Network-RBFN and Neural Network-NN algorithm in [63]. This developed method has been compared with traditional methods. It has been tested at different temperatures and irradiance values. MPPT algorithms using HC and ANFIS techniques have been examined in [64]. A hybrid MPPT algorithm has been developed using several different methods that work more efficiently in changing atmospheric conditions. Since the processing load of ANN algorithms is high, they force microprocessors in terms of processing time. For this reason, an ANN-based MPPT algorithm has been developed

using FPGA in reference [65]. In [66], [67], the success of ANN algorithm has been shown in capturing GMP point under partial shading conditions. In SI technique in which a mathematical model of the system is obtained by using the input and output values of a system, photovoltaic power systems have been used in the modeling of many different systems such as Ankle Joint Dynamic Stiffness, Unmanned Surface Vessel and DC-DC converter [68], [73]. In [74], the mathematical model of the system was obtained for the design of the control algorithm developed by Bao *et al.* To control the voltage in a power distribution system using SI, in [75], an online-SI technique consisting of state estimation module, collision avoidance module, excitation module and parameter estimation module for underwater robotic vehicles has been developed by George *et al.* In [87], a fast-converging MPPT algorithm based on Modified Butterfly Optimization Algorithm was proposed. The proposed algorithm had the ability that could distinguish among partial shading patterns, uniform shading, solar intensity, and load change conditions. It was experimentally verified by using SEPIC converter. An improvement was achieved by 99.85% in partial shading, 47.20% in uniform shading, and 86.15% under sudden load variations.

Hybrid MPPT methods have been developed as a result of using conventional and advanced methods to increase the performance of existing methods. Some of the current hybrid methods are as follows: Firefly algorithm with incremental conductance (IC-FFA), perturb & observe with adaptive neural network (PO-ANN), fireworks algorithm with perturb & observe (FWA-PO), gray wolf with perturb & observe (GWO-PO), bat search algorithm with perturb & observe (BSA-PO), particle swarm optimization with perturb & observe (PSO-PO), simulated annealing with particle swarm optimization (SA-PSO), fish swarm algorithm with particle swarm optimization (FSA-PSO), jaya algorithm with differential evolution (JA-DE), whale optimization with differential evolution (WO-DE), particle swarm optimization with shuffled frog leaping algorithm (PSO-SFLA) [6], simulated annealing and perturb & observe (SA-PO) [12], differential evolution with particle swarm optimization (DE-PSO), ant colony optimization with perturb & observe (ACO-PO) [76], artificial neural network with sequential monte carlo (ANN-SMC), modified genetic algorithm and firefly algorithm (MGA-FFA), taguchi method and genetic algorithm (T-GA), augmented state feedback precise linearization and artificial neural network (AFL-ANN), artificial bee colony and perturb & observe algorithm (ABC-PO) [13].

The advantages and disadvantages of each MPPT algorithm in terms of complexity, oscillation, number of sensors, cost and dependency on PV Array are summarized in Table 1.

These developed methods differ in terms of application, accuracy, complexity, and efficiency. These techniques are also summarized in different sources numbered [6], [12], [17], [39], [77], [78], [79] in the literature.

III. THE BEHAVIOUR OF PV SYSTEM

MP point of PV power system is constantly changing depending on the atmospheric conditions [80], [81]. The angle of incidence of sunlight, dusting, partial shading, irradiance intensity, and temperature are among the reasons that create these changing atmospheric conditions. As the amount of irradiance increases under constant temperature, the current generation capacity of the panel increases significantly. However, this situation does not create the same increase in panel voltage. As the temperature increases under constant irradiance, the photovoltaic current generated by the panel increases slightly, but this significantly reduces the panel voltage. Monitoring MP point of PV system that exhibits non-linear behavior under these variable conditions is inevitable in terms of efficiency. The variation of the power obtained from PV system concerning time is expressed by Eq.(1) [79].

$$P_{PV}(t) = F\{V_{PV}(t), I_{PV}(t), \gamma(t)\} \quad (1)$$

Here, V_{PV} stands for panel output voltage, I_{PV} for panel output current, and γ for all other PV system parameters and climatic variables. The dynamic behavior of PV systems is different under i) uniform irradiance and ii) partial shading. Therefore, PV system and MPPT algorithms to be developed should be analyzed and developed according to these two different concepts.

A. UNDER UNIFORM IRRADIANCE CONDITION

Large-scale PV systems consist of identical panels connected in series and parallel to each other. PV panels are connected in series to increase the voltage of the array and in parallel to increase the output current [13]. The same output current and output power are obtained from all identical panels exposed to the same irradiance. The characteristic behavior of a PV panel can be explained easily with the help of I-V and P-V curves. When PV system is under uniform irradiance, a single GMP point is formed on I-V and P-V curves.

Fig.1 shows I-V and P-V curves under STC of a 10 kW PV system. All the panels in PV system are exposed to the same amount of irradiance. Because of this, a single GMP point is formed on both curves as shown in Fig.1. The system operates with higher efficiency at this point. It is easy to find MP point of PV system under uniform irradiance. If the measurements are correct, MP point can be found with high accuracy. Conventional MPPT techniques have higher performance under uniform irradiance.

B. UNDER PARTIAL SHADING CONDITION

Due to their large surface area, both PV panels and PV power systems can be exposed to different intensities of irradiance depending on dusting, clouding, and other atmospheric conditions. Different output currents and output power are obtained from each of the identical panels exposed to different irradiance. In this case, multiple local LMP points occur in PV system.

In Fig.2, I-V and P-V curves of the 10 kW PV system under PSC are shown. Since all arrays in the PV system are exposed

TABLE 1. Comparison of different MPPT algorithms.

Classification	Algorithm	Reference	Complexity	Sensors	Oscillation	Cost	DPVA
Conventional	PO	[20, 22]	Low	I, V	High	Medium	No
	IC	[50, 51, 52]	Medium	I, V	High	Medium	No
	CVR	[23, 53, 54]	Low	I	Medium	Low	No
	ARV	[17, 24]	Low	I, V	Medium	Low	No
	CC	[25, 26]	Low	V	Low	Low	No
	HC	[27, 28, 58]	Low	I, V	High	Medium	No
	PC	[29, 34]	Low	I, V	Medium	High	No
	FOCV	[30, 77]	Low	I, V	Low	Low	No
	FSCC	[31, 77]	Low	I, V	Low	Low	No
RCC	[32, 34]	High	I, V	Medium	High	No	
Advanced	ANN	[65, 66]	High	I, V	Low	High	No
	FLC	[15, 17, 55]	Medium	I, V, P	Medium	High	No
	PSO	[4, 16]	Medium	I, V	Medium	High	No
	IPSO	[6, 13]	High	I, V	Low	High	No
	GA	[23, 39]	Medium	I, V	Medium	High	No
	GWO	[12, 17]	High	I, V	Low	High	No
	ABC	[11, 12]	Low	I, V	Medium	Low	Yes
	ACO	[12, 15]	Low	I, V	Medium	Low	No
	FFA	[14, 16]	Medium	I, V	Low	Medium	No
	DE	[11, 39]	Medium	I, V	Medium	Medium	No
	BSA	[39]	High	I, V	Low	High	No
	CA	[39]	High	I, V	Low	High	No
	JA	[39]	Medium	I, V	Medium	Medium	Yes
	GSA	[14]	High	I, V	Low	Medium	No
	MKE	[13]	High	I, V	Low	Medium	No
	CS	[9, 12]	Medium	I, V	Low	Medium	Yes
	BOA	[13]	Medium	I, V	Low	Medium	No
	MFO	[14]	Medium	I, V	Low	Medium	No
	SSA	[14]	Medium	I, V	Low	High	No
	SFLA	[6, 13]	High	I, V	Low	High	No
	FSA	[9, 17]	Medium	I, V, P	Low	High	No
	CSO	[14]	High	I, V	Low	High	No
	WDO	[13]	Low	I, V	Medium	High	No
	BA	[14]	High	I, V	Medium	High	Yes
	CSA	[12, 15]	High	I, V	Medium	High	No
	SSM	[13]	High	I, V	Low	Medium	Yes
	RSM	[13]	High	I, V	Low	Low	Yes
	PS	[13]	Medium	I, V	Medium	Medium	No
	GSS	[13]	High	I, V	Medium	High	Yes
	ESC	[12]	High	I, V	High	Medium	No
	BN	[14, 15]	High	I, V	Low	High	Yes
	MRL	[13]	High	I, V	Low	High	No
	TRL	[13]	High	I, V	Low	High	No
	MPTA	[14]	High	I, V	Low	Medium	Yes
	ESA	[14, 19]	High	I, V	Medium	Medium	Yes
	CSR	[13]	High	I, V	Medium	High	Yes
	TS	[13]	Medium	I, V, P	Medium	Low	No
	AV	[14]	Medium	I, V, P	Low	High	No
	OCC	[13]	Low	I, P	Low	Medium	No
	SCS	[13]	Low	I, V	Low	Medium	No
SA	[10, 12]	High	I, V	Medium	Low	Yes	
FWA	[13]	Medium	I, V	Low	Medium	Yes	
FPA	[76]	Medium	I, V	Low	High	No	
TLBO	[13]	Medium	I, V	Low	High	No	
MBA	[13]	Medium	I, V	Medium	Medium	No	
WO	[13]	Medium	I, V	Medium	High	No	
HPO	[13]	Low	I, V	Low	High	No	

TABLE 1. (Continued.) Comparison of different MPPT algorithms.

Hybrid	SI-ARV	[57]	High	V, T	Low	High	No
	IC-FFA	[6, 13]	Medium	I, V	Low	Medium	No
	PO-ANN	[13]	High	I, V	Low	High	No
	FWA-PO	[13]	Medium	I, V	Low	Medium	Yes
	GWO-PO	[12]	Medium	I, V	Low	Medium	No
	BSA-PO	[6, 13]	Medium	I, V	Medium	Medium	No
	PSO-PO	[12]	Medium	I, V	Low	High	No
	SA-PSO	[13]	Medium	I, V	Medium	High	No
	FSA-PSO	[13]	High	I, V, P	Medium	High	Yes
	JA-DE	[13]	High	I, V	Low	High	No
	WO-DE	[13]	High	I, V	Medium	High	Yes
	PSO-SFLA	[13]	High	I, V, P	Low	High	No
	SA-PO	[12]	High	I, V	Medium	Low	Yes
	DE-PSO	[12, 76]	Medium	I, V	Low	Low	Yes
	ACO-PO	[76]	Low	I, V	Medium	Medium	No
	ANN-SMC	[14]	High	I, V	Low	High	No
	MGA-FFA	[14]	Medium	I, V	Medium	Medium	Yes
	T-GA	[14]	Medium	I, V, P	Medium	Medium	Yes
	AFL-ANN	[13]	High	I, V	Low	High	No
	ABC-PO	[13]	Medium	I, V	Low	High	No
ANN-PSO	[14]	High	I, V	Low	High	No	

DPVA - Dependency on PV Array ; T – Temperature ; I – Current ; V- Voltage ; P - Power

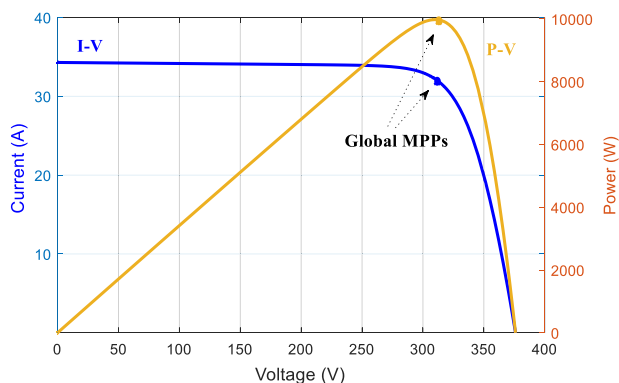


FIGURE 1. Characteristic I-V/P-V curves of the PV system under STC.

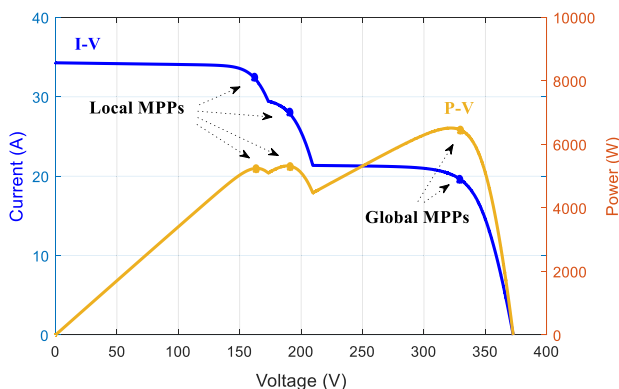


FIGURE 2. Characteristic I-V/P-V curves of the PV system under PSC.

to different intensities of irradiance, more than one local LMP point has been formed as shown in the Fig.2. The PV system

works with lower efficiency at these points [80], [81]. It is much more difficult to find the GMP point since there is more than one MP point, local and global, in the PV system under PSC. Compared to uniform irradiance, more sophisticated MPPT techniques with higher technology are needed for partial shading. Advanced and hybrid MPPT techniques developed for this show high performance under partial shading conditions.

C. PV PANEL MODEL

PV cells have a nonlinear structure and act as a current source. The electrical circuit model of a PV cell is shown in Fig.3. This model consists of a current source I_{PV} , a diode connected in reverse and parallel to this current source, and an R_S resistor connected in series with a parallel R_P resistor [82], [83]. This model is known as a single diode model.

$$I = I_{PV} - I_0 \left(\exp\left(\frac{V + R_S I}{a}\right) - 1 \right) - \frac{V + R_S I}{R_P} \quad (2)$$

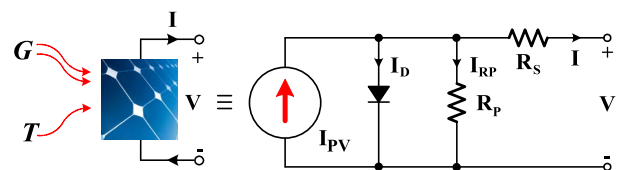


FIGURE 3. Electrical equivalent circuit model of the PV cell.

Here, I_{PV} represents the current produced in PV cell by the photoelectric effect depending on the T temperature and G irradiance and it is expressed as in Eq.(3).

$$I_{PV} = (I_{PV,n} + K_I(T - T_n)) \frac{G}{G_n} \quad (3)$$

$I_{PV,n}$, refers to the current produced by n number of parallel cells, T_n refers to the nominal panel temperature in Kelvin, G refers to the irradiance value at the panel surface (W/m^2) and G_n refers to the nominal irradiance value (W/m^2). The saturation current of the diode I_0 is a function of the temperature. It is expressed as in Eq.(4).

$$I_0 = \frac{I_{SC,n} + K_I(T - T_n)}{\exp(\frac{V_{OC,n} + K_V(T - T_n)}{a}) - 1} \quad (4)$$

$$a = \frac{N_S n k T}{q} \quad (5)$$

Since equation (2) contains exponential terms, I-V and P-V curves of PV cell are also nonlinear. V_{OC} on I-V curve given in Fig.4 represents open circuit voltage of the cell, I_{SC} represents short circuit current of the cell and MPP represents the maximum power point. PV cell can only produce maximum power at this MPP point. All developed MPPT algorithms ensure that PV system operates with high efficiency at a steady state by continuously monitoring MP point.

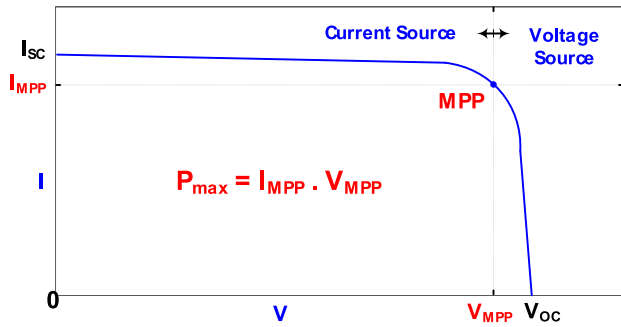


FIGURE 4. I-V characteristic curve of PV cell.

IV. SYSTEM IDENTIFICATION METHODOLOGY

The controller design is an important subject in control systems. The mathematical model of the physical system is needed for design. System Identification-SI is used for creating an approximate mathematical model of the system using real input-output data of physical systems. Since the mathematical model of linear systems with specific parameters can be easily obtained, it is easy to design a controller for these systems. However, mathematical modeling of physical systems with uncertain nonlinear parameters and the design of the controller for the control process through this non-linear model is more complex. Physical systems are divided into 3 in terms of parameter uncertainty. These are named white-box, gray-box, and black-box systems, as shown in Fig.5 [69], [84].

The model in which all system parameters are known is called the white-box system. In the model, some features of the system are known. However, some of them are determined by the data obtained from the system is the gray-box model. Black-box systems, on the other hand, are systems with uncertain parameters. However, they have no information about their contents. The mathematical model of

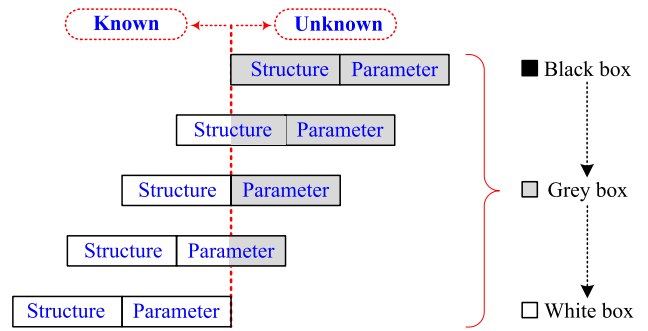


FIGURE 5. Dynamical system classifications by structures and parameters.

black-box systems is created by analyzing the input-output data obtained from empirical studies on the system in the time-domain or frequency-domain level [85].

For black-box systems, different linear and nonlinear modeling techniques have been developed, classified as in Fig. 6 [69].

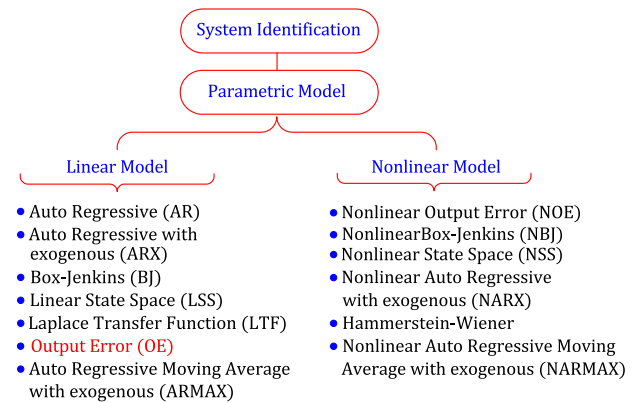


FIGURE 6. System identification modeling techniques.

These techniques are used in various systems for control and prediction. Different system identification techniques can be preferred for varying systems. With system identification, linear models such as transfer functions, process models, polynomial models, and state-space models can be obtained by using time-domain, time series, or frequency-domain data. Using only time-domain data, nonlinear models such as NARX and Hammerstein-Wiener can be predicted. The modeling process with system identification consists of the steps in the flow diagram given in Fig.7 [86].

In the first step, the input-output data obtained through the empirical way, are prepared. In the second step, a modeling technique suitable for the model is selected from the techniques given in Fig.6. Choosing the modeling technique is one of the most difficult steps in the modeling process. Since, there are many possibilities.

The best performing model structure is selected among these many possibilities by comparison. In the third step, the accuracy of the selected model structure is tested by evaluating its behavior with a validation data set that has not

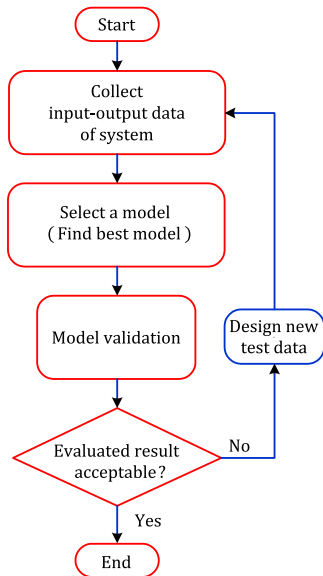


FIGURE 7. Flowchart for system identification methodology.

been used before. In the fourth step, if the evaluation result is within acceptable limits, the system identification process is terminated. If not, the modeling process is reset with new test data.

V. PROPOSED SI-BASED POLYNOMIAL ARV-MPPT TECHNIQUE

In this study, a MPPT technique that is based on system identification was proposed. Modeling was carried out assuming that the analyzed PV system is a nonlinear black-box system. The input-output data required for modeling were created in the MATLAB/Simulink platform. Then, by using these data in the system identification toolbox platform, the mathematical model of PV system in a polynomial structure giving the relationship $y(t) = V_{ref}/T$ was obtained.

Here, T is the model input as temperature information, and V_{ref} is the model output as the generated reference voltage. As it is known, the output voltages of PV panels vary slightly with the irradiance values, but show greater changes depending on the ambient temperature. T-V curve expressing the relationship between temperature and voltage and G-V curve expressing the relationship between irradiance and voltage are shown together in Fig.8. These curves are obtained when the system is open circuit and all the PV panels in the system are exposed to the same intensity of temperature and irradiance changes.

The change amount in V_{PV} , which is the open-circuit voltage of each PV array that constitutes the 10 kW PV power system used in this study, was obtained as follows with the help of Fig.8:

- The string voltage obtained at G-V curve / $T = 25\text{ }^\circ\text{C}$ constant temperature and irradiance values of $[100\text{-}1000\text{ W/m}^2]$ are $V_{PV\text{-min}}=341\text{V}$ and $V_{PV\text{-max}} = 376\text{V}$. The amount of change due to irradiance is about 9.3%.

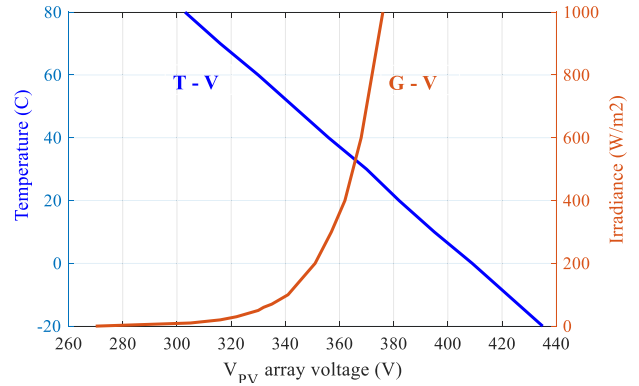


FIGURE 8. T-V and G-V curves of 10 kW PV system.

- The string voltage obtained under T-V curve / $G=1000\text{ W/m}^2$ constant irradiance and temperatures $[-20\text{ }^\circ\text{C}, +80\text{ }^\circ\text{C}]$ are $V_{PV\text{-min}}=303\text{V}$ and $V_{PV\text{-max}}=435\text{V}$. The change amount depending on the temperature is approximately 30.3%.

As you can see, because of $\frac{|V_{PV\text{-max}} - V_{PV\text{-min}}|_{G\text{-V curve}}}{|V_{PV\text{-max}} - V_{PV\text{-min}}|_{T\text{-V curve}}} < 1$, for a simpler design, only the ambient temperature T is used as input for the polynomial model. The estimated output of the polynomial model is the reference voltage called V_{ref} .

PV cells have a nonlinear structure. In this study, it was aimed to estimate the voltage at MP point by using both a simplified PV system model and a smaller number of sensors. For this purpose, a simplified polynomial model of a PV system with a nonlinear structure was obtained, and simulations were made. The obtained polynomial model has a “discrete-time output error (OE)” polynomial structure. Higher performance can be achieved by creating models with more complex structures. However, its ease of implementation and simple structure is the superiorities of this proposed polynomial model.

The purpose of this study is to develop a high-performance MPPT algorithm by simplifying the previously developed complex models. For this purpose, as a preliminary study, analyses were performed creating three and higher-order models with different polynomial structures by using System Identification. When the results obtained for the 10 kW PV system were examined, it was observed that the performance of the high-order polynomial models was not much higher or it was lower than the performance of the second-order polynomial model. In this regard, the second-order polynomial model structure was preferred due to both simplicity and high performance.

The polynomial model expresses the relationship between input-output and disruptive factors as a transfer function by using the mathematical structure of the system. The generalized polynomial model is expressed as in Eq.(6):

$$A(q)y(t) = \sum_{i=1}^{nu} \frac{B_i(q)}{F_i(q)} u_i(t - nk_i) + \frac{C(q)}{D(q)} e(t) \quad (6)$$

The variables A, B, C, D, F in Eq. (6) are polynomials expressed in the time shift operator q^{-1} . Here, u_i is the i^{th} input, n_u is the total number of inputs and nk_i is the i^{th} input delay. Also, $e(t)$ represents noise with the variance of λ .

The polynomial model obtained in this study has a discrete-time output error (OE) polynomial structure. The simplest form of this structure is given in Eq. (7).

$$y(t) = \frac{B(z)}{F(z)}u(t) + e(t) \tag{7}$$

Here $y(t)$ represents the output voltage V_{ref} and $u(t)$ represents the system input temperature T . As a result, $B(z)$ and $F(z)$ terms were obtained with system identification toolbox as in Eq.(8) to obtain the V_{ref} voltage:

$$\left. \begin{aligned} B(z) &= 0.7336z^{-1} + 0.743z^{-2} \\ F(z) &= 1 - 1.006z^{-1} + 0.01293z^{-2} \end{aligned} \right\} \tag{8}$$

The sampling time was determined as 0.01s and 15001 pieces of data were used to obtain the terms, $B(z)$ and $F(z)$. The temperature-dependent polynomial transfer function model of the PV system is given in Fig.9.

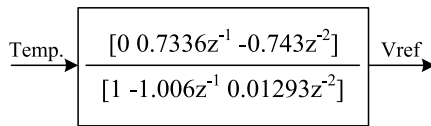


FIGURE 9. The temperature-dependent polynomial transfer function model of the PV system.

This polynomial model has been used to obtain the reference voltage V_{ref} within the proposed MPPT algorithm. The error obtained by comparing the output voltage of the PV system with this reference voltage is processed by a PI controller, hence the “ d ” duty ratio is determined. Thus, the power produced by PV system under changing atmospheric conditions is transferred to the output with maximum efficiency, and the voltage at the ends of the load is kept constant by the boost converter driven with d duty ratio. The block diagram of the proposed SI-based ARV-MPPT method is given in Fig.10. A polynomial transfer function block obtained by the system identification method consists of a PI controller and a different block.

The proposed method provides impressive performance in both fast and slow changes of temperature and irradiance. The reference voltage produced by SI-based ARV-MPPT method is also an adaptive method as it adapts to changing atmospheric conditions. Once the model is created, using only the temperature as input is sufficient to obtain the V_{ref} voltage. While obtaining “ d ” duty ratio, it is sufficient to measure the panel output voltage.

Current measurement is not required in the method. In this respect, an advantage has been achieved in terms of the number of sensors compared to many studies. SI-based ARV-MPPT method proposed in this article is a hybrid method consisting of the synthesis of SI methodology with the conventional ARV method. Depending on the resolution and

min-max values of temperature and irradiance data sets applied to the model input during the training phase, the optimum reference voltage is obtained at the model output.

The model proposed for a 10 kW system in this study can also be easily improved for higher power PV systems where all input-output data can be monitored. Unlike other studies, using the system identification methodology, this article provides an opportunity to conduct feasibility studies of large-scale PV systems by modeling them in the computer environment before the installation stage to reduce the whole system to a single polynomial model, conduct performance tests, and reveal behavioral models for different climatic conditions.

VI. MODELING OF PV POWER SYSTEM

The modeled PV power system has the configuration shown in Fig.11. PV power system consists of 40 panels connected in series and parallel, DC-DC boost converter, and MPPT block. As shown in Table 2, PV arrays were connected in series with 10 Trina Solar TSM-250PA05.08 model PV modules, and 4 of these arrays were connected in parallel to create the power stage of the PV system. The panel, boost converter, and all other system parameters related to the PV power system are explained in Table 3.

VII. SIMULATION MODEL

The simulation model of PV system created in MATLAB/Simulink with MPPT method suggested in this study is given in Fig.12. The sampling frequency is determined as $5\mu s$, and the switching frequency for the boost converter is 20 kHz. The fact that the sampling frequency of the simulation model is higher than the switching frequency allows obtaining results that are closer to reality.

To test the effectiveness of the proposed MPPT method, 2 separate simulations were carried out by creating 2 separate scenarios as shown in Fig.13a-b. Temperature and irradiance change graphs of scenario-2 are given in Fig.13b, and scenario-1 is shown in Fig.13a.

Scenario-1 represents atmospheric conditions in which temperature changes slowly and irradiance changes both rapidly and slowly, while scenario-2 represents atmospheric conditions in which temperature and irradiance change rapidly. In both scenarios, all 40 panels in PV system are simultaneously exposed to an equal amount of temperature and irradiance change. Depending on these changes, MP point is constantly changing. Although MP point is constantly changing, a single global MP point is formed on the power curve of the PV system because the entire PV system is exposed to a regular amount of temperature and irradiance.

In both scenarios, all simulation results obtained by testing the performance of the proposed SI-based polynomial ARV method and PO, IC, CVR, ANN-based ARV, and SI-based nonlinear ARV methods are comparatively given in graphs. The simulation model, where all MPPT methods are performed under equal conditions and the results are obtained, is given in Fig.14.

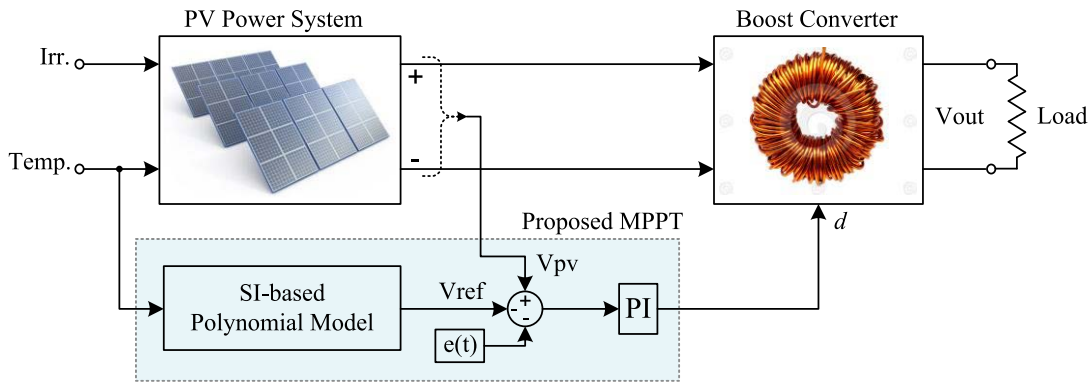


FIGURE 10. Block diagram of the proposed SI-based polynomial ARV-MPPT method.

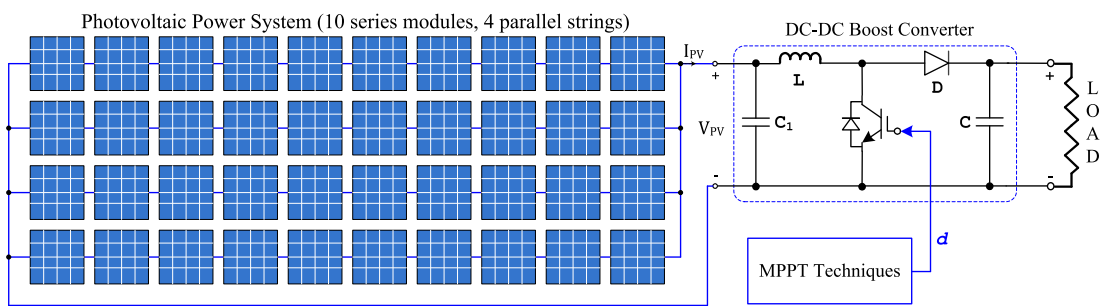


FIGURE 11. 10 kW PV power system.

TABLE 2. Configuration of the PV power system.

	Label	Module	Pmax, W
Parallel	Array-1	10 series-connected PV Modules, Trina Solar TSM-250PA05.08	2498.6
	Array-2	10 series-connected PV Modules, Trina Solar TSM-250PA05.08	2498.6
	Array-3	10 series-connected PV Modules, Trina Solar TSM-250PA05.08	2498.6
	Array-4	10 series-connected PV Modules, Trina Solar TSM-250PA05.08	2498.6
		Total Power	9994.4

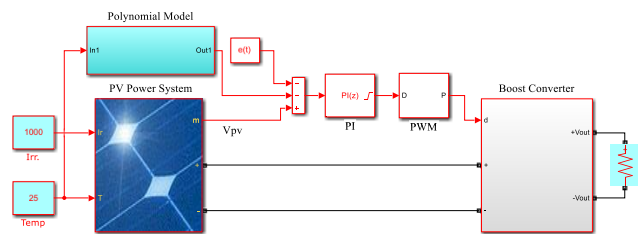


FIGURE 12. Simulation model of the proposed SI-based polynomial ARV-MPPT method.

VIII. ANALYSIS AND COMPARISON

The graphs of current, voltage, and power obtained from the PV power system using all MPPT methods under changing atmospheric conditions in Scenario-1 are given in Figs. 15-21. Fig.15 shows the change graphs of the output voltage V_{PV} of the PV power system. In region 2, PO method followed MP point correctly by overexposing.

The IC method, on the other hand, could not catch the MP point. In region number 1, where the irradiance shows a sinusoidal change, the excessive decrease in voltages obtained by PO and IC is shown in detail in Fig.16. With the proposed SI-based polynomial ARV method, a more correct voltage has been obtained in the entire working range. SI-based polynomial ARV, SI-based nonlinear ARV, and ANN-based ARV graphics display similar behavior, although they have less fluctuation compared to other graphics. However, since the proposed method has a simpler structure than both methods, it can be easily performed with microprocessors in practice.

In Fig.17, there are graphs of the change of I_{PV} currents from the PV power system. The current generation capacity of the PV system depends on the amount of irradiance and the form of change. In this respect, the current waveforms are in the same form as the irradiance change given in scenario 1. However, there are deviations in PO and IC currents in the 1st region, a decrease in IC and CVR

TABLE 3. Parameters of PV power system.

	Symbol	Quantity	Values	
PV Module	P_{MPP}	Maximum power at MPP	250	W
	V_{MPP}	Voltage at MPP	31	V
	I_{MPP}	Current at MPP	8.06	A
	V_{OC}	Open-circuit voltage	37.6	V
	I_{SC}	Short-circuit current	8.55	A
	$T_C@V_{OC}$	Temp. coefficient of Voc	-0,35	%/°C
	$T_C@I_{SC}$	Temp. coefficient of Isc	0,06	%/°C
	R_S	Series resistance of the PV cell	0,247	Ω
	R_P	Parallel resistance of the PV cell	301,814	Ω
	N_{cell}	Cells per module	60	-
Boost Converter	N_{sm}	Number of series module	10	-
	N_{pm}	Number of parallel module	4	-
	L	Boost inductor	5e-5	H
	C	Boost capacitor	2000e-6	F
	C_I	Boost input capacitor	3e-3	H
	f_{SW}	Switching frequency	20	kHz
	V_{IN}	Input voltage range of boost conv.	355-375	V
	P_{LOAD}	Load value	10	kW
	T_S	Simulation step time	5e-6	s

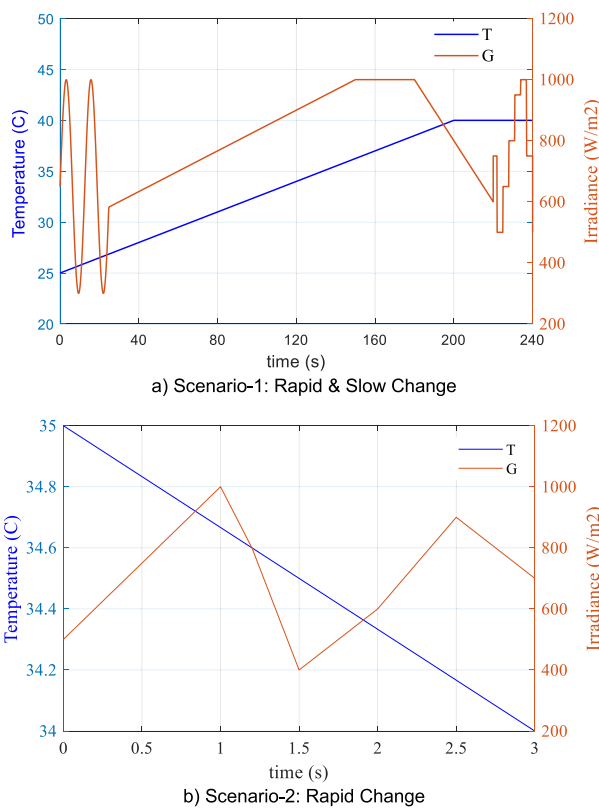


FIGURE 13. Variable atmospheric scenarios.

currents in the 2nd and 3rd region, and high oscillations in PO current. All MPPT methods behave similarly depending on the irradiance change in the 200s and 4th region, where the temperature remains constant and the irradiance changes.

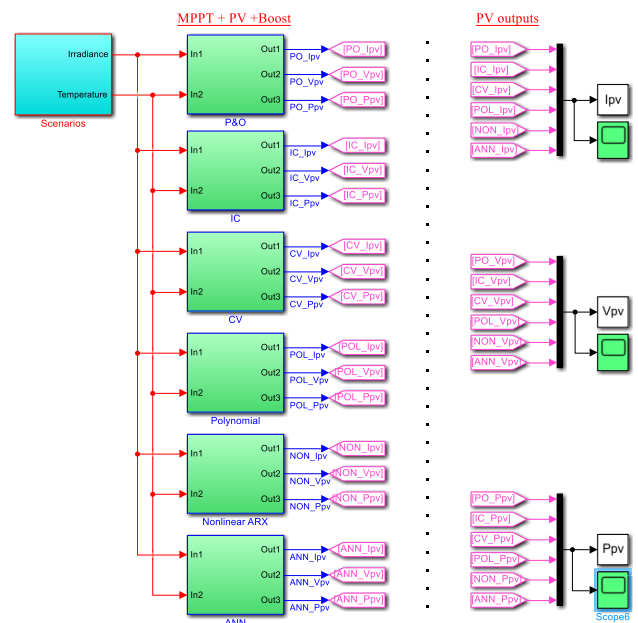


FIGURE 14. Implementation model for all MPPT techniques.

However, as shown in Fig.18, the current waveform obtained with the proposed SI-based polynomial ARV during the simulation period [0-240s] is more correct.

In Fig.19 and Fig.20, the enlarged versions of voltage and current graphs obtained for Scenario-1 are given. As seen, the voltage and current obtained by the proposed SI-based polynomial ARV show a smooth change in the given range. Especially high oscillations occur in PO and IC graphs.

In Fig.21, P_{PV} power change graphs drawn from the PV power system are given. The waveforms are in the same

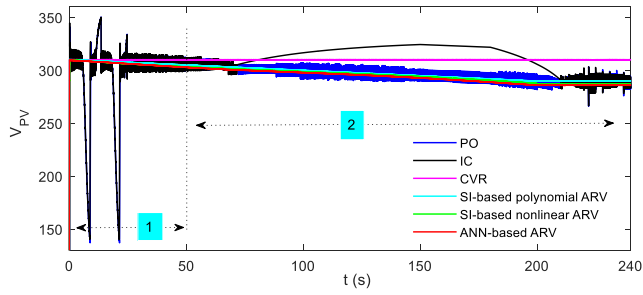


FIGURE 15. V_{PV} graphs for all MPPTs under scenario-1.

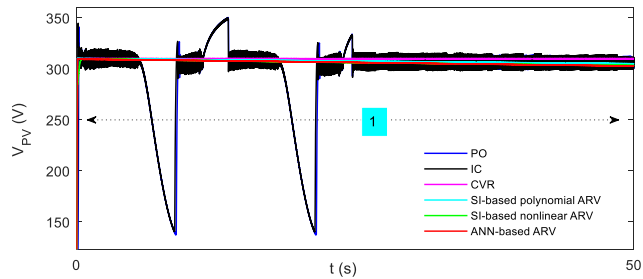


FIGURE 16. V_{PV} graphs for all MPPTs under scenario-1 [0-50s].

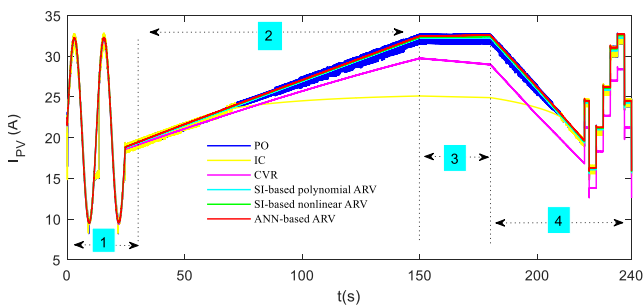


FIGURE 17. I_{PV} graphs for all MPPTs under scenario-1.

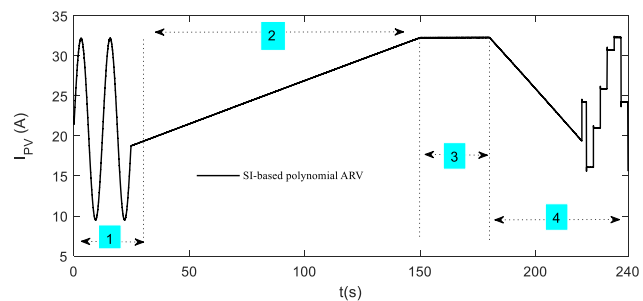


FIGURE 18. I_{PV} graph for SI-based polynomial ARV-MPPT under scenario-1.

form as the irradiance change given in scenario-1. With the proposed method, a smoother power without oscillation was obtained by monitoring the MP point with high performance in all operating ranges. This situation can be seen more clearly in SI-based polynomial ARV-MPPT graph given in Fig.22. In Fig.23, the transient state graphs of P_{PV} for 6 different regions in the range of [0-240s] are given in detail.

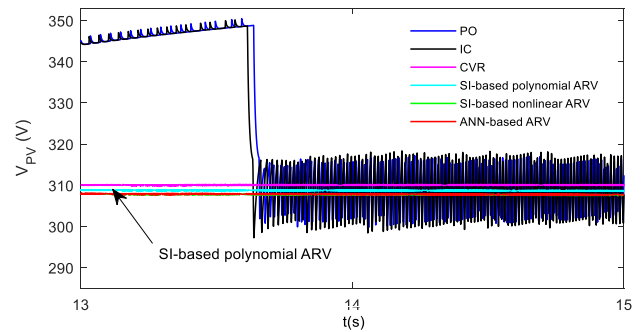


FIGURE 19. V_{PV} graphs for all MPPTs under scenario-1 [13-15s].

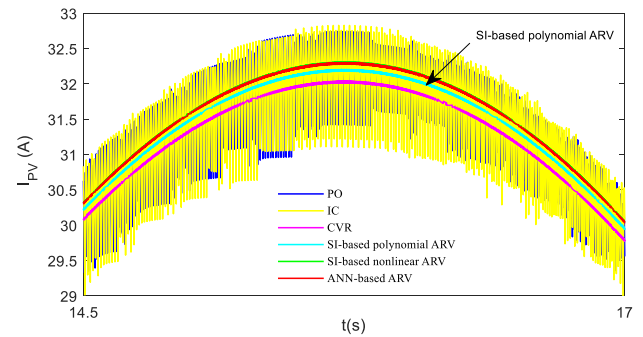


FIGURE 20. I_{PV} graphs for all MPPTs under scenario-1 [14.5-17s].

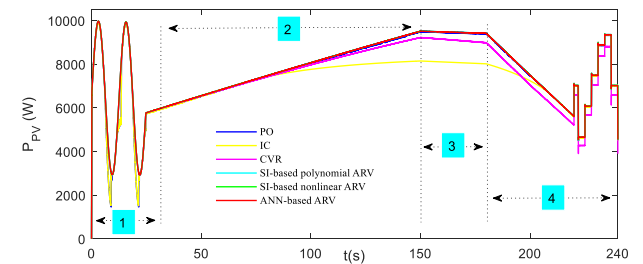


FIGURE 21. P_{PV} graphs for all MPPTs under scenario-1.

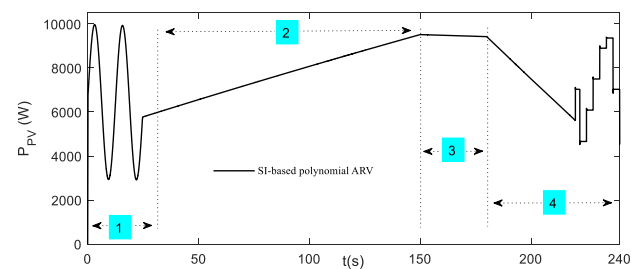


FIGURE 22. P_{PV} graph for SI-based polynomial ARV-MPPT under scenario-1.

The graphs of current, voltage, and power obtained from the PV power system by using all MPPT methods under variable atmospheric conditions in the range of [0-3s] in Scenario-2 are given in Figs.24-30. The temperature is decreasing steadily. Irradiance, on the other hand, has

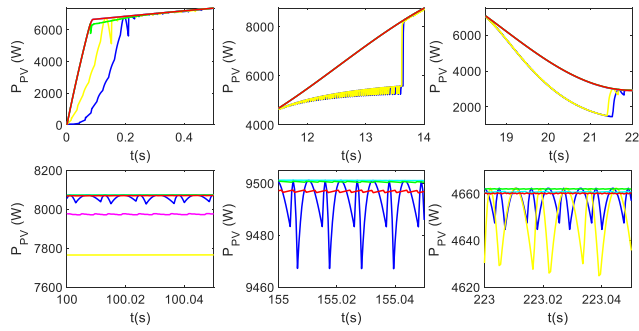


FIGURE 23. P_{PV} transient state graphs under scenario-1.

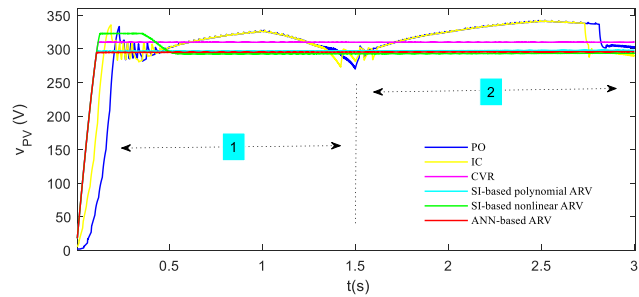


FIGURE 24. V_{PV} graphs for all MPPTs under scenario-2.

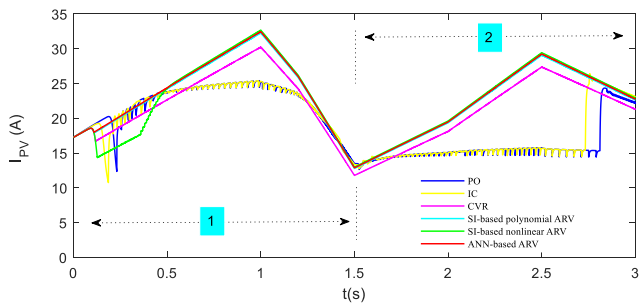


FIGURE 25. I_{PV} graphs for all MPPTs under scenario-2.

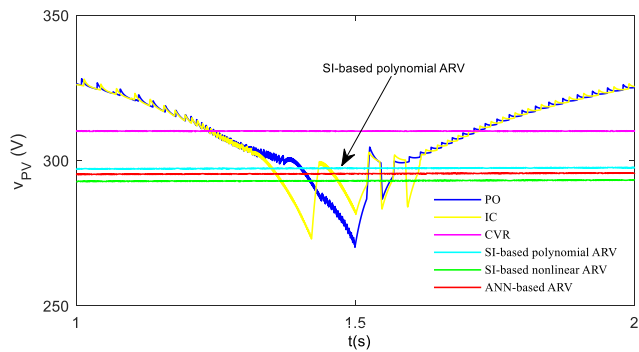


FIGURE 26. V_{PV} graphs for all MPPTs under scenario-2 [1-2s].

increased and decreased in regions 1 and 2. Temperature change has occurred 3 times faster than Scenario-1. The change graphs of V_{PV} output voltages obtained from the PV power system under this rapid change are shown in Fig.24.

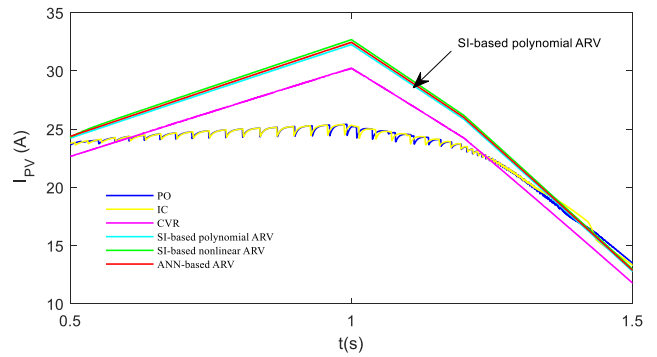


FIGURE 27. I_{PV} graphs for all MPPTs under scenario-2 [0.5-1.5s].

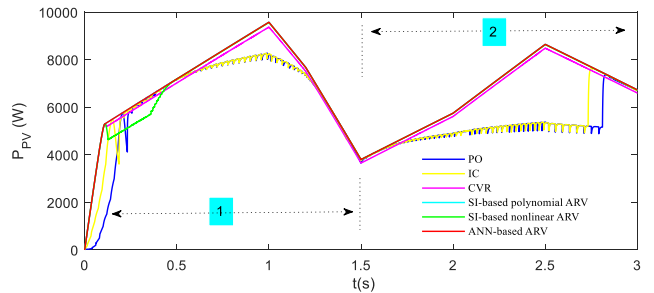


FIGURE 28. P_{PV} graphs for all MPPTs under scenario-2.

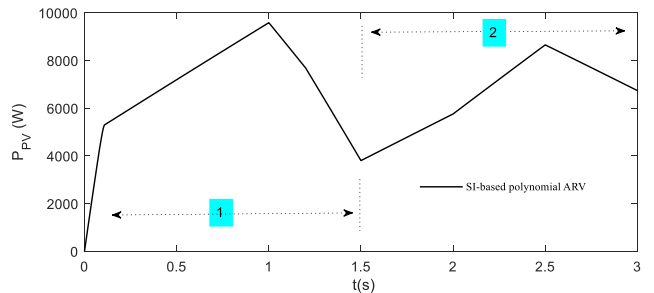


FIGURE 29. P_{PV} graph for SI-based polynomial ARV-MPPT under scenario-2.

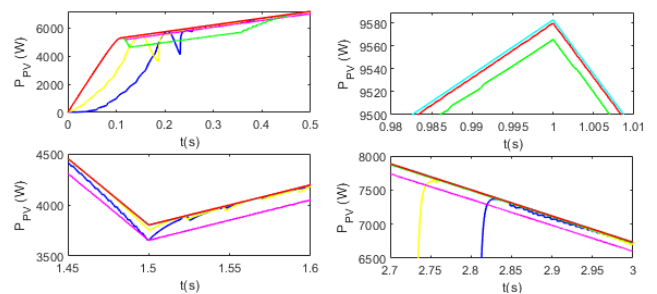


FIGURE 30. P_{PV} transient state graphs under scenario-2.

As can be seen from these graphs, V_{PV} voltage obtained with SI-based polynomial ARV is stable and smooth, despite the rapid change of temperature and irradiance in both the 1st and 2nd regions. SI-based nonlinear ARV and ANN-based ARV methods have also behaved similarly. In SI-based polynomial

TABLE 4. Performance assessment of PO, IC, CVR, ANN-ARV, SI-ARV and SI-POL ARV.

Case	Region	t (s)	G (W/m ²)	T (°C)	Algorithm	Power (W)	Voltage (V)	Current (A)
Scenario-1	Region-1	21.30	321	26.6	PO	1560	142.40	10.955
					IC	1550	141.50	10.954
					CVR	3125	309.90	10.083
					ANN-ARV	3137	306.70	10.228
					SI-ARV	3138	307.90	10.191
					SI-pol ARV	3140	306.70	10.238
	Region-2	145	983.4	38.88	PO	9364	291.30	32.145
					IC	8127	324.00	25.083
					CVR	9108	310.10	29.371
					ANN-ARV	9372	293.50	31.931
					SI-ARV	9374	294.60	31.819
					SI-pol ARV	9376	295.40	31.740
	Region-3	170	1000	37.75	PO	9414	288.40	32.642
					IC	8062	322.70	24.982
					CVR	9070	310.20	29.239
					ANN-ARV	9448	290.40	32.534
					SI-ARV	9453	291.60	32.417
					SI-pol ARV	9455	292.70	32.302
	Region-4	235	1000	40	PO	9318	285.80	32.603
					IC	9325	285.90	32.616
CVR					8799	310.00	28.383	
ANN-ARV					9348	285.90	32.696	
SI-ARV					9355	287.20	32.573	
SI-pol ARV					9361	289.80	32.301	
Scenario-2	Region-1	1	1000	34.67	PO	8224	326.30	25.203
					IC	8255	326.00	25.322
					CVR	9362	310.10	30.190
					ANN-ARV	9570	295.20	32.418
					SI-ARV	9556	292.60	32.658
					SI-pol ARV	9573	296.90	32.243
	Region-2	2	600	34.33	PO	4907	325.00	15.098
					IC	4884	325.40	15.009
					CVR	5614	310.20	18.098
					ANN-ARV	5754	295.50	19.472
				SI-ARV	5750	293.30	19.604	
				SI-pol ARV	5757	297.40	19.357	

t:Time; G:Irradiance; T:Temperature

ARV method, the transition to perpetual state is smoother. Since PO and IC methods are not adaptive methods, the voltages associated with these methods are highly affected by the change of irradiance.

The photovoltaic effect and current generation capacity of panels are directly proportional to the amount of irradiance falling on the panel surfaces and their change. This situation is seen in the current graphs in Fig.25. Despite the changes in atmospheric conditions, the maximum current was obtained from the PV power system with the proposed SI-based polynomial ARV, SI-based nonlinear ARV, ANN-based ARV, and CVR methods. It is the change in irradiance that determines the waveforms of these currents. However, currents obtained by PO and IC methods could not react to the change in the increase and decrease in irradiance at the same rate. With these two methods, as in the proposed SI-based polynomial ARV method, the maximum current could not be obtained

from the PV system. Due to their adaptive nature, currents obtained with SI-based polynomial ARV, SI-based nonlinear ARV, and ANN-based ARV are similar.

In Fig.26 and Fig.27, the enlarged versions of voltage and current graphs obtained for Scenario-2 are given. As seen, the voltage obtained by the proposed SI-based polynomial ARV shows a smooth change in the given range.

Power charts drawn from the PV system are given in Fig.28. It has a similar form to the current graphs, depending on the change of atmospheric conditions in Scenario-2. Maximum power was obtained from the PV system with the recommended method SI-based polynomial ARV at all points between these values with 1000 W/m² where the irradiance value is the highest and 400 W/m² where it is the lowest. However, the maximum power point could not be reached with PO and IC methods in 1000 W/m² irradiance. Therefore, the superior performance of the proposed SI-based

polynomial ARV method in tracking MP point is seen in Fig.29.

In Fig.30, the transient state graphs of P_{PV} for 4 different regions in the range of [0-3s] are given in detail. In all working areas under variable atmospheric conditions, the maximum utilization of the PV system was made with the proposed method.

Detailed power, voltage and current data for different regions in all two scenarios are shown in Table 4.

IX. CONCLUSION

In reference voltage-based MPPT methods, estimating the model of the PV system showing nonlinear behavior with high accuracy directly affects the performance of the method. In this respect, all PV system parameters must be known or measurable to obtain a high accuracy model. However, in practice, some of these parameters are not measurable. Therefore, different modeling techniques should be used for systems with parameter uncertainty.

In this study, an adaptive reference voltage-based MPPT method has been developed. The reference voltage is estimated with SI-based polynomial model created by the black box modeling method of the PV power system whose MP point will be monitored. The nonlinear model obtained is independent of the actual physical parameters of the PV system. Therefore, there is no need to estimate or measure the actual system parameters during the modeling process. While creating the model, only the input variables of the PV system, temperature, and the output variable, voltage data were used. Once the polynomial model is created in this way regardless of the system parameters, the only temperature is used as the model input. Also, there is no need for current measurement during model creation or application. This is an advantage of the proposed method in terms of the number of sensors and cost.

Also, the problem of capturing MP point, which occurs because of temperature change, has been eliminated. Therefore, the superior performance of the proposed reference voltage-based MPPT method in tracking the MP point under variable atmospheric conditions compared to other methods has been proven by the simulation results obtained. Current, voltage and power fluctuations around the MP point are minimized.

In industrial applications, there are many PV system installations with different parameters and different powers. In this study, this modeling method is suggested for a 10 kW system; and the obtained polynomial model can be developed for PV systems with the higher power. In the future, this modeling method will provide great convenience in large-scale PV systems. That is to say, the measured input-output data of large-scale PV systems can be monitored with central SCADA systems, modeling can be made on these data without the need for detailed field measurements, and MPPT and controller designs can be realized.

The proposed SI-based polynomial ARV-MPPT method is practically applicable since it includes a polynomial and a

PI controller. Thanks to its simple and inexpensive structure, it can be easily performed with low-level microprocessors. A more effective system model can be developed by optimizing the coefficients and degree of the polynomial model.

REFERENCES

- [1] *Renewables 2019 Global Status Report (Paris: REN21 Secretariat)*, document REN21, 2019.
- [2] *Renewables 2019 Global Status Report (Paris: REN21 Secretariat)*, document REN21, 2020.
- [3] H. Zhang, Z. Lu, W. Hu, Y. Wang, L. Dong, and J. Zhang, "Coordinated optimal operation of hydro-wind-solar integrated systems," *Appl. Energy*, vol. 242, pp. 883–896, May 2019.
- [4] S. Obukhov, A. Ibrahim, A. A. Z. Diab, A. S. Al-Sumaiti, and R. Aboelsaud, "Optimal performance of dynamic particle swarm optimization based maximum power trackers for stand-alone PV system under partial shading conditions," *IEEE Access*, vol. 8, pp. 20770–20785, 2020.
- [5] R. Venkateswari and S. Sreejith, "Factors influencing the efficiency of photovoltaic system," *Renew. Sustain. Energy Rev.*, vol. 101, pp. 376–394, Mar. 2019.
- [6] F. Belhachat and C. Larbes, "A review of global maximum power point tracking techniques of photovoltaic system under partial shading conditions," *Renew. Sustain. Energy Rev.*, vol. 92, pp. 513–553, Sep. 2018.
- [7] D. Rekioua and E. Matagne, *Optimization of Photovoltaic Power Systems-Modelization, Simulation and Control*. London, U.K.: Springer-Verlag, 2012, pp. 115–116.
- [8] A. Yazdani and P. P. Dash, "A control methodology and characterization of dynamics for a photovoltaic (PV) system interfaced with a distribution network," *IEEE Trans. Power Del.*, vol. 24, no. 3, pp. 1538–1551, Jul. 2009.
- [9] L. Liu, X. Meng, and C. Liu, "A review of maximum power point tracking methods of PV power system at uniform and partial shading," *Renew. Sustain. Energy Rev.*, vol. 53, pp. 1500–1507, Jan. 2016.
- [10] S. Lyden and M. E. Haque, "Maximum power point tracking techniques for photovoltaic systems: A comprehensive review and comparative analysis," *Renew. Sustain. Energy Rev.*, vol. 52, pp. 1504–1518, Dec. 2015.
- [11] M. A. Ramli, S. Twaha, K. Ishaque, and Y. A. Al-Turki, "A review on maximum power point tracking for photovoltaic systems with and without shading conditions," *Renew. Sustain. Energy Rev.*, vol. 67, pp. 144–159, Jan. 2017.
- [12] A. Mohapatra, B. Nayak, P. Das, and K. B. Mohanty, "A review on MPPT techniques of PV system under partial shading condition," *Renew. Sustain. Energy Rev.*, vol. 80, pp. 854–867, Dec. 2017.
- [13] B. Yang, T. Zhu, J. Wang, H. Shu, T. Yu, X. Zhang, W. Yao, and L. Sun, "Comprehensive overview of maximum power point tracking algorithms of PV systems under partial shading condition," *J. Cleaner Prod.*, vol. 268, pp. 1–24, Sep. 2020.
- [14] F. Belhachat and C. Larbes, "Comprehensive review on global maximum power point tracking techniques for PV systems subjected to partial shading conditions," *Sol. Energy*, vol. 183, pp. 476–500, May 2019.
- [15] G. Dileep and S. N. Singh, "Application of soft computing techniques for maximum power point tracking of SPV system," *Sol. Energy*, vol. 141, pp. 182–202, Jan. 2017.
- [16] G. Li, Y. Jin, M. W. Akram, X. Chen, and J. Ji, "Application of bio-inspired algorithms in maximum power point tracking for PV systems under partial shading conditions—A review," *Renew. Sustain. Energy Rev.*, vol. 81, pp. 840–873, Jan. 2018.
- [17] R. B. Bollipo, S. Mikkili, and P. K. Bonthagorla, "Critical review on PV MPPT techniques: Classical, intelligent and optimisation," *IET Renew. Power Gener.*, vol. 14, no. 9, pp. 1433–1452, 2020.
- [18] M. Abdel-Salam, M.-T. El-Mohandes, and M. Goda, "An improved perturb-and-observe based MPPT method for PV systems under varying irradiation levels," *Sol. Energy*, vol. 171, pp. 547–561, Sep. 2018.
- [19] J. Ahmed and Z. Salam, "An enhanced adaptive P&O MPPT for fast and efficient tracking under varying environmental conditions," *IEEE Trans. Sustain. Energy*, vol. 9, no. 3, pp. 1487–1496, Jul. 2018.
- [20] K. H. Hussein, I. Muta, T. Hoshino, and M. Osakada, "Maximum photovoltaic power tracking: An algorithm for rapidly changing atmospheric conditions," *IEE Proc.-Gener. Transm. Distrib.*, vol. 142, no. 1, pp. 59–64, 1995.
- [21] S. Bhattacharyya, S. Kumar, and B. Singh, "Adaptive damped circular current limit control for PV grid-tied system," *IEEE Trans. Ind. Appl.*, vol. 56, no. 2, pp. 1197–1204, Mar. 2020.

- [22] G. J. Yu, Y. S. Jung, J. Y. Choi, I. Choy, J. H. Song, and G. S. Kim, "A novel two-mode MPPT control algorithm based on comparative study of existing algorithms," in *Proc. Conf. Rec. 29th IEEE Photovoltaic Specialists Conf.*, Apr. 2002, pp. 1531–1534.
- [23] M. Lasheen, A. K. A. Rahman, M. Abdel-Salam, and S. Ookawara, "Performance enhancement of constant voltage based MPPT for photovoltaic applications using genetic algorithm," *Energy Proc.*, vol. 100, pp. 217–222, Nov. 2016.
- [24] M. Lasheen, A. K. A. Rahman, and M. Abdel-Salam, "Adaptive reference voltage-based MPPT technique for PV applications," *IET Renew. Power Gener.*, vol. 11, no. 5, pp. 715–722, Mar. 2017.
- [25] X. Di, M. Yundong, and C. Qianhong, "A global maximum power point tracking method based on interval short-circuit current," in *Proc. 16th Eur. Conf. Power Electron. Appl.*, Aug. 2014, pp. 1–8.
- [26] Z. M. Salameh, F. Dagher, and W. A. Lynch, "Step-down maximum power point tracker for photovoltaic systems," *Sol. Energy*, vol. 46, no. 5, pp. 279–282, 1991.
- [27] S. B. Kjær, "Evaluation of the 'hill climbing' and the 'incremental conductance' maximum power point trackers for photovoltaic power systems," *IEEE Trans. Energy Convers.*, vol. 27, no. 4, pp. 922–929, Oct. 2012.
- [28] X. Xiao, X. Huang, and Q. Kang, "A hill-climbing-method-based maximum-power-point-tracking strategy for direct-drive wave energy converters," *IEEE Trans. Ind. Electron.*, vol. 63, no. 1, pp. 257–267, Jan. 2016.
- [29] A. Brambilla, M. Gambarara, A. Garutti, and F. Ronchi, "New approach to photovoltaic arrays maximum power point tracking," in *Proc. 30th Annu. IEEE Power Electron. Spec. Conf. Rec.*, Jul. 1999, pp. 632–637.
- [30] Y.-P. Huang, "A rapid maximum power measurement system for high-concentration photovoltaic modules using the fractional open-circuit voltage technique and controllable electronic load," *IEEE J. Photovolt.*, vol. 4, no. 6, pp. 1610–1617, Nov. 2014.
- [31] T. Noguchi, S. Togashi, and R. Nakamoto, "Short-current pulse-based maximum-power-point tracking method for multiple photovoltaic-and-converter module system," *IEEE Trans. Ind. Electron.*, vol. 49, no. 1, pp. 217–223, Feb. 2002.
- [32] P. Sahu, A. Sharma, and R. Dey, "Ripple correlation control maximum power point tracking for battery operated PV systems: A comparative analysis," in *Proc. IEEE Int. IoT, Electron. Mechatronics Conf. (IEMTRON-ICS)*, Sep. 2020, pp. 1–6.
- [33] S. R. Mohamed, P. Aruna Jeyanthi, D. Devaraj, M. H. Shwehdi, and Adel Aldalbahi, "DC-link voltage control of a grid-connected solar photovoltaic system for fault ride-through capability enhancement," *Appl. Sci.*, vol. 9, pp. 1–27, Jan. 2019.
- [34] B. Subudhi and R. Pradhan, "A comparative study on maximum power point tracking techniques for photovoltaic power systems," *IEEE Trans. Sustain. Energy*, vol. 4, no. 1, pp. 89–98, Jan. 2013.
- [35] I. H. Altas and A. M. Sharaf, "A novel on-line MPP search algorithm for PV arrays," *IEEE Trans. Energy Convers.*, vol. 11, no. 4, pp. 748–754, Dec. 1996.
- [36] V. R. Kota and M. N. Bhukya, "A simple and efficient MPPT scheme for PV module using 2-dimensional lookup table," in *Proc. IEEE Power Energy Conf. Illinois (PECI)*, Feb. 2016, pp. 1–7.
- [37] A. Ovono Zue and A. Chandra, "State feedback linearization control of a grid connected photovoltaic interface with MPPT," in *Proc. IEEE Electr. Power Energy Conf. (EPEC)*, Oct. 2009, pp. 1–6.
- [38] M. Guisser, E. Abdelmounim, M. Aboulfatah, and A. Eljouni, "Nonlinear inputoutput feedback linearization mppt control based on state observer for a photovoltaic pumping system," in *Proc. 1er Colloque Franco-Marocain Sur Les Énergies Nouvelles et Renouvelables*, 2014, pp. 1–7.
- [39] A. O. Baba, G. Liu, and X. Chen, "Lassification and evaluation review of maximum power point tracking methods," *Sustain. Futures*, vol. 2, pp. 1–28, Jan. 2020.
- [40] M. DebBarma, S. Deb, and C. Nandi, "Maximum photovoltaic power tracking using perturb & observe algorithm in MATLAB/simulink environment," *Int. J. Electr. Eng. Technol.*, vol. 1, no. 1, pp. 71–84, 2010.
- [41] J. Ahmed and Z. Salam, "An improved perturb and observe (P&O) maximum power point tracking (MPPT) algorithm for higher efficiency," *Appl. Energy*, vol. 150, pp. 97–108, Jul. 2015.
- [42] T. H. Kwan and X. Wu, "High performance P&O based lock-on mechanism MPPT algorithm with smooth tracking," *Sol. Energy*, vol. 155, pp. 816–828, Oct. 2017.
- [43] J. Ahmed and Z. Salam, "A modified P&O maximum power point tracking method with reduced steady-state oscillation and improved tracking efficiency," *IEEE Trans. Sustain. Energy*, vol. 7, no. 4, pp. 1506–1515, Oct. 2016.
- [44] A. Belkaid, I. Colak, and K. Kayisli, "Implementation of a modified P&O-MPPT algorithm adapted for varying solar radiation conditions," *Electr. Eng.*, vol. 99, no. 3, pp. 839–846, Sep. 2017.
- [45] K. Ishaque, Z. Salam, and G. Lauss, "The performance of perturb and observe and incremental conductance maximum power point tracking method under dynamic weather conditions," *Appl. Energy*, vol. 119, pp. 228–236, Apr. 2014.
- [46] T. Radjai, L. Rahmani, S. Mekhilef, and J. P. Gaubert, "Implementation of a modified incremental conductance MPPT algorithm with direct control based on a fuzzy duty cycle change estimator using dSPACE," *Sol. Energy*, vol. 110, pp. 325–337, Dec. 2014.
- [47] A. Loukriz, M. Haddadi, and S. Messalti, "Simulation and experimental design of a new advanced variable step size incremental conductance MPPT algorithm for PV systems," *ISA Trans.*, vol. 62, pp. 30–38, May 2016.
- [48] M. E. Başoğlu and B. Çakir, "An improved incremental conductance based MPPT approach for PV modules," *TURKISH J. Electr. Eng. Comput. Sci.*, vol. 23, pp. 1687–1697, Nov. 2015.
- [49] F. Liu, S. Duan, B. Liu, and Y. Kang, "A variable step size inc MPPT method for PV systems," *IEEE Trans. Ind. Electron.*, vol. 55, no. 7, pp. 2622–2628, Jul. 2008.
- [50] K. S. Tey and S. Mekhilef, "Modified incremental conductance algorithm for photovoltaic system under partial shading conditions and load variation," *IEEE Trans. Ind. Electron.*, vol. 61, no. 10, pp. 5384–5392, Oct. 2014.
- [51] L. Xu, R. Cheng, and J. Yang, "A modified INC method for PV string under uniform irradiance and partially shaded conditions," *IEEE Access*, vol. 8, pp. 131340–131351, 2020.
- [52] M. Alsumiri, "Residual incremental conductance based nonparametric MPPT control for solar photovoltaic energy conversion system," *IEEE Access*, vol. 7, pp. 87901–87906, 2019.
- [53] Z. Ye and X. Wu, "Compensation loop design of a photovoltaic system based on constant voltage MPPT," in *Proc. Asia-Pacific Power Energy Eng. Conf.*, Mar. 2009, pp. 1–4.
- [54] Y. Xiong, S. Qian, and J. Xu, "Research on constant voltage with incremental conductance MPPT method," in *Proc. Asia-Pacific Power Energy Eng. Conf.*, Mar. 2012, pp. 1–4.
- [55] R. Kumar and Y. K., "Comparative study of MPPT methods for solar PV driven induction motor load," *Int. J. Comput. Appl.*, vol. 127, no. 5, pp. 37–44, Oct. 2015.
- [56] N. Rebei, A. Hmidet, R. Gammoudi, and O. Hasnaoui, "Implementation of photovoltaic water pumping system with MPPT controls," *Frontiers Energy*, vol. 9, no. 2, pp. 187–198, Jun. 2015.
- [57] R. Celikel and A. Gundogdu, "System identification-based MPPT algorithm for PV systems under variable atmosphere conditions using current sensorless approach," *Int. Trans. Electr. Energy Syst.*, vol. 30, no. 8, pp. 1–21, Aug. 2020.
- [58] V. K. Devi, K. Premkumar, A. B. Beevi, and S. Ramaiyer, "A modified perturb & observe MPPT technique to tackle steady state and rapidly varying atmospheric conditions," *Sol. Energy*, vol. 157, pp. 419–426, Nov. 2017.
- [59] R. Celikel, "ANN based angle tracking technique for shaft resolver," *Measurement*, vol. 148, Dec. 2019, Art. no. 106910.
- [60] O. Aydogmus and G. Boztas, "Deep learning-based approach for speed estimation of a PMA-SynRM," in *Proc. 11th Int. Conf. Electr. Electron. Eng. (ELECO)*, Nov. 2019, pp. 172–176.
- [61] R. Celikel, "Speed control of BLDC using NARMA-L2 controller in single link manipulator," *Balkan J. Electr. Comput. Eng.*, vol. 7, no. 2, pp. 143–148, Apr. 2019.
- [62] E. Deniz, "ANN-based MPPT algorithm for solar PMSM drive system fed by direct-connected PV array," *Neural Comput. Appl.*, vol. 28, no. 10, pp. 3061–3072, Oct. 2017.
- [63] S. Saravanan and N. R. Babu, "RBFN based MPPT algorithm for PV system with high step up converter," *Energy Convers. Manage.*, vol. 122, pp. 239–251, Aug. 2016.
- [64] M. Lasheen and M. Abdel-Salam, "Maximum power point tracking using Hill climbing and ANFIS techniques for PV applications: A review and a novel hybrid approach," *Energy Convers. Manage.*, vol. 171, pp. 1002–1019, Sep. 2018.
- [65] P. Q. Dzung, L. D. Khoa, H. H. Lee, L. M. Phuong, and N. T. D. Vu, "The new MPPT algorithm using ANN-based PV," in *Proc. Int. Forum Strategic Technol.*, Oct. 2010, pp. 402–407.
- [66] S. A. Rizzo and G. Scelba, "ANN based MPPT method for rapidly variable shading conditions," *Appl. Energy*, vol. 145, pp. 124–132, May 2015.

- [67] R. Khanaki, M. A. M. Radzi, and M. H. Marhaban, "Artificial neural network based maximum power point tracking controller for photovoltaic standalone system," *Int. J. Green Energy*, vol. 13, no. 3, pp. 283–291, Feb. 2016.
- [68] P. Manganiello, M. Ricco, G. Petrone, E. Monmasson, and G. Spagnuolo, "Optimization of perturbative PV MPPT methods through online system identification," *IEEE Trans. Ind. Electron.*, vol. 61, no. 12, pp. 6812–6821, Dec. 2014.
- [69] A. Alqahtani, S. Marafi, B. Musallam, and N. E. D. A. El Khalek, "Photovoltaic power forecasting model based on nonlinear system identification," *Can. J. Electr. Comput. Eng.*, vol. 39, no. 3, pp. 243–250, 2016.
- [70] K. Jalaaladini, E. S. Tehrani, and R. E. Kearney, "A subspace approach to the structural decomposition and identification of ankle joint dynamic stiffness," *IEEE Trans. Biomed. Eng.*, vol. 64, no. 6, pp. 1357–1368, Jun. 2017.
- [71] J. Shin, D. J. Kwak, and Y.-I. Lee, "Adaptive path-following control for an unmanned surface vessel using an identified dynamic model," *IEEE/ASME Trans. Mechatronics*, vol. 22, no. 3, pp. 1143–1153, Jun. 2017.
- [72] N. Beohar, V. N. K. Malladi, D. Mandal, S. Ozev, and B. Bakkaloglu, "Online built-in self-test of high switching frequency DC–DC converters using model reference based system identification techniques," *IEEE Trans. Circuits Syst. I, Reg. Papers*, vol. 65, no. 2, pp. 818–831, Feb. 2018.
- [73] M. Al-Greer, M. Armstrong, M. Ahmeid, and D. Giaouris, "Advances on system identification techniques for DC–DC switch mode power converter applications," *IEEE Trans. Power Electron.*, vol. 34, no. 7, pp. 6973–6990, Jul. 2019.
- [74] Y. Bao, L. Y. Wang, C. Wang, and Y. Wang, "Hammerstein models and real-time system identification of load dynamics for voltage management," *IEEE Access*, vol. 6, pp. 34598–34607, 2018.
- [75] G. C. Karras, P. Marantos, C. P. Bechlioulis, and K. J. Kyriakopoulos, "Unsupervised online system identification for underwater robotic vehicles," *IEEE J. Ocean. Eng.*, vol. 44, no. 3, pp. 642–663, Jul. 2018.
- [76] J. P. Ram and N. Rajasekar, "A new global maximum power point tracking technique for solar photovoltaic (PV) system under partial shading conditions (PSC)," *Energy*, vol. 118, no. 1, pp. 512–525, Jan. 2017.
- [77] R. Ahmad, A. F. Murtaza, and H. A. Sher, "Power tracking techniques for efficient operation of photovoltaic array in solar applications—A review," *Renew. Sustain. Energy Rev.*, vol. 101, pp. 82–102, Mar. 2019.
- [78] M. A. Danandeh and S. M. G. Mousavi, "Comparative and comprehensive review of maximum power point tracking methods for PV cells," *Renew. Sustain. Energy Rev.*, vol. 82, pp. 2743–2767, Feb. 2018.
- [79] N. Karami, N. Moubayed, and R. Outbib, "General review and classification of different MPPT techniques," *Renew. Sustain. Energy Rev.*, vol. 68, pp. 1–18, Feb. 2017.
- [80] D. Verma, S. Nema, A. M. Shandilya, and S. K. Dash, "Maximum power point tracking (MPPT) techniques: Recapitulation in solar photovoltaic systems," *Renew. Sustain. Energy Rev.*, vol. 54, pp. 1018–1034, Feb. 2016.
- [81] S. R. Pendem and S. Mikkili, "Modeling, simulation, and performance analysis of PV array configurations (series, series-parallel, bridge-linked, and honey-comb) to harvest maximum power under various partial shading conditions," *Int. J. Green Energy*, vol. 15, no. 13, pp. 795–812, Oct. 2018.
- [82] O. Aydogmus, "Design of a solar motor drive system fed by a direct-connected photovoltaic array," *Adv. Electr. Comput. Eng.*, vol. 12, no. 3, pp. 53–58, 2012.
- [83] A. Gundogdu and R. Celikel, "ANN-based MPPT algorithm for photovoltaic systems," *Turkish J. Sci. Technol.*, vol. 15, no. 2, pp. 101–110, 2020.
- [84] N. Patcharaprakiti, K. Kirtikara, K. Tunlasakun, J. Thongpron, D. Chenvidhya, A. Sangswang, V. Monyakul, and B. Muenpinij, *Modeling of Photovoltaic Grid Connected Inverters Based on Nonlinear System Identification for Power Quality Analysis*. China: InTech, 2011, pp. 1–33, doi: 10.5772/16914.
- [85] A. Gundogdu, R. Celikel, and O. Aydogmus, "Comparison of Si-ANN and extended Kalman filter-based sensorless speed controls of a DC motor," *Arabian J. Sci. Eng.*, vol. 46, no. 2, pp. 1241–1256, Feb. 2021.
- [86] S. A. Zulkeflee, S. A. Sata, and N. Aziz, *Nonlinear Autoregressive With Exogenous Inputs Based Model Predictive Control for Batch Citronellol Laurus Esterification Reactor*. China: InTech, 2011, pp. 1–27, doi: 10.5772/16963.
- [87] I. Shams, S. Mekhilef, and K. S. Tey, "Maximum power point tracking using modified butterfly optimization algorithm for partial shading, uniform shading, and fast varying load conditions," *IEEE Trans. Power Electron.*, vol. 36, no. 5, pp. 5569–5581, May 2021.
- [88] T. K. Soon and S. Mekhilef, "Modified incremental conductance MPPT algorithm to mitigate inaccurate responses under fast-changing solar irradiation level," *Sol. Energy*, vol. 101, pp. 333–342, Mar. 2014.
- [89] T. K. Soon and S. Mekhilef, "A fast-converging MPPT technique for photovoltaic system under fast-varying solar irradiation and load resistance," *IEEE Trans. Ind. Informat.*, vol. 11, no. 1, pp. 176–186, Feb. 2015.



AHMET GUNDOĐDU received the M.Sc. degree in electrical teaching and the Ph.D. degree in electrical engineering from the University of Firat, Elazığ, Turkey, in 2004 and 2012, respectively. From 2000 to 2012, he was a Research Assistant with the Department of Electrical Teaching. Since 2013, he has been an Assistant Professor with the Department of Electrical Engineering, Batman University. His research interests include magnetic levitation, electrical machines, motor control, motor driver, and PV systems.

• • •